Journal of Macromolecular Science, Part A
Publication details, including instructions for authors and subscription information:
http://www.informaworld.com/smpp/title~content=t713597274

Synthesis of Novel Semiconducting Aromatic Polyesteramids Containing Pyridine: Characterization of Nanometer-Sized Rod-Like Analogues and their Copper (II) Complexes

Hammed H. A. M. Hassan[a]; Amel F. Elhusseiny[a]; Amr M. Sweyllam[b]
[a] Chemistry Department, Faculty of Science, Alexandria University, Ibrahimia, Alexandria, Egypt [b] Physics department, Faculty of Science, Alexandria University, Moharrem Bee, Alexandria, Egypt

Online publication date: 26 April 2010

To cite this Article Hassan, Hammed H. A. M. , Elhusseiny, Amel F. and Sweyllam, Amr M.(2010) 'Synthesis of Novel Semiconducting Aromatic Polyesteramids Containing Pyridine: Characterization of Nanometer-Sized Rod-Like Analogues and their Copper (II) Complexes', Journal of Macromolecular Science, Part A, 47: 6, 521 — 533
To link to this Article: DOI: 10.1080/10601321003741909
URL: http://dx.doi.org/10.1080/10601321003741909

Journal of Macromolecular Science, Part A: Pure and Applied Chemistry (2010) **47**, 521–533

ISSN: 1060-1325 print / 1520-5738 online
DOI: 10.1080/10601321003741909

Taylor & Francis
Taylor & Francis Group

Synthesis of Novel Semiconducting Aromatic Polyesteramids Containing Pyridine: Characterization of Nanometer-Sized Rod-Like Analogues and their Copper (II) Complexes

HAMMED H. A. M. HASSAN[1,*], AMEL F. ELHUSSEINY[1,**] and AMR M. SWEYLLAM[2,***]

[1]*Chemistry Department, Faculty of Science, Alexandria University, Ibrahimia, Alexandria, Egypt*
[2]*Physics Department, Faculty of Science, Alexandria University, Moharrem Bee, Alexandria, Egypt*

Received October 2009, Accepted December 2009

In this paper, new thermally stable isomeric unsubstituted polyesteramides have been successfully prepared by condensation of aromatic acids chlorides namely; isophthaloyl, pyridine-3,5-dicarbonyl and pyridine-2,6-pyridine-dicarbonyl dichlorides with the aminophenol isomers in NMP. Conducting the reaction in NMP/H_2O (90/10 v/v) followed by centrifugal separation furnished the desired polymers as rod-like nanoparticles. The morphology of obtained nanoparticles were studied by SEM. Mixing NMP with H_2O was essential for controlling the particles morphology and as a reaction accelerator.

Pyridine-containing polymers exhibit semi-conducting nature as their conductivities increase with increasing temperature, while no variation of the conductivity with the temperature was observed for their corresponding phenylene analogues. Introduction of the nitro group into the polymer backbone led to a red shift in the absorption and the obtained polymers have a bright yellow color, which is unusual with this polymer group. Copper (II) ions were complexed the polyesteramides-containing nitro group in a (1:1) ratio. Complexes of pyridine-containing polymers exhibit semiconducting nature changed to metallic characters on heating and their conductivities increased tens of magnitudes than their corresponding ligands. These new types of polymeric materials and their nano-sized rods may have numerous applications in nanotechnology and their properties can be tuned for specific applications such as conducting adhesives and coating materials.

Keywords: Nanorodes, polyesteramides, morphology, structure-property relations, polymer metal complex

1 Introduction

High-performance-heat resistance polymers such as aromatic polyimides, poly(amide-imide)s, polyamides and polyesters are characterized by their excellent balance of thermal and mechanical properties which makes them useful materials for engineering applications. The great commercial importance and the fabrication of such unsubstituted polymers are owing to two reasons (1); i) they proved to be thermally stable (2) and, unlike other polymer types, they show a tendency to decompose during or even before melting, ii) they are insoluble in most common solvents. Major elements that account for the low solubility are molecular order and strong interchain attractive forces, mainly hydrogen bonding (3) that enhances effective molecular packing. Moreover, the high moisture absorptions have resulted in obvious negative effect on their mechanical properties (4), as well as electrical insulating and dielectric performance.

Many efforts have been made to create structurally modified aromatic polymers having increased solubility and processability with retention of their high thermal stability (5–7). Modification of the properties of polymer by incorporation of hydrogen-bonded polyester groups has been investigated and polyesteramides have been studied extensively (8–11). The materials are either random copolymers in which the proportion of ester-to-amide groups can be varied through the whole range of compositions, or alternating or patterned polyesteramides with regularly recurring successions of the characteristic groups in the main chain. The alternating or patterned polyesteramides are obtained by the polyesterification of amide-containing or the polyamidation of ester containing precursors (12). Segmented polyesteramides consisting of rigid amide segments and amorphous flexible ester segments are thermoplastic elastomers (13). These polymers have a micro-phase separated structure with an amide-rich hard phase and an

*Address correspondence to: Hammed H. A. M. Hassan, Chemistry Department, Faculty of Science, Alexandria University, P. O. Box 426-Ibrahimia, Alexandria 21321, Egypt. Tel: +2 012 5888 595; Fax: +203 39 11 794; E-mail: hassan10@safwait.com
**Tel: +2 017 7766 645; Fax: +203 39 11 794; E-mail: dr_amelfawzy@yahoo.com
***Tel: +203 5777 330; Fax: +203 39 11 794; E-mail: sweyllam1@yahoo.fr

ester-rich soft phase. The amide-rich phase usually contains crystalline lamellae and acts as a thermo reversible physical cross-linker for the amorphous phase. The soft phase has a sub-ambient glass transition temperature (T_g) and contributes to the flexibility and extensibility of the polymer. Heating above the melting temperature of the hard domains usually results in phase mixing of hard and soft segments. Previous research revealed that an effective way to improve phase separation is using short, symmetrical and uniform amide blocks (14–17).

A part of an active project based on synthesis and characterization of aromatic polyamides and polyesteramides containing pyridyl linkages to develop novel semiconducting nanoparticles made from organic polyamides and their metallic complexes, we report the preparation of novel polyesteramids containing pyridine via polycondensation of aromatic diacid chlorides with aminophenol isomers. Furthermore, condensation with 5-nitro-2-aminophenol was investigated in order to understand to what extent may insertion of a strong electron-withdrawing group such as (NO_2) group change in the electronic and vibrational spectra of the investigated polymers (18). For structure-property comparison reasons, nanoscale preparation of three examples of polyesteramides and their copper (II) complex were investigated (19). One of the most important tasks in our study is to analyze and predict the detailed polymer structures that could increase the thermal stability, which directly affect processing and practical application. It is interesting to correlate the structure-property relationship, in particular, studying the influence of the pyridine N-atom position on the polymer properties. In this way, *n*-electrons of the pyridine N-atom are either incorporated in the linear conjugation or not and this may induce the least detrimental effect on the electrical properties of the produced polymer (20).

2 Experimental

2.1 Materials

Isophthaloyl dichloride **1** (Fig. 1), pyridine-2,6-dicarbonyl dichloride **2** and pyridine-3,5-dicarbonyl dichloride **3**, were made from the commercial isophthalic acid (Merck), pyridine-2,6-dicarboxylic acid (Aldrich), pyridine-3,5-dicarboxylic acid (Aldrich), respectively, following the literature procedures (21). The commercial aminophenols **4-7**, hydrated cupric acetate and the solvents *N*, *N*-dimethylacetamide (DMAc), 1-Methyl-2-pyrrolidone (NMP) (Fluka), 1,4-dioxane (Aldrich) and dimethylsulfoxide (DMSO) (Aldrich) were used as purchased without purification.

2.2 Measurements

Infrared spectra (IR, KBr pellets; 3 mm thickness) were recorded on a Perkin-Elmer Infrared Spectrophotometer (FTIR 1650). All spectra were recorded within the wave number range of 4000–600 cm^{-1} at 25°C. Absorption spectra were measured with a UV 500 UV(-)Vis spectrometer at room temperature (rt) in DMSO with a polymer concentration of 2 mg/10 mL. Differential thermo gravimetric (DTG) analyses were carried out in the temperature range from 20°C to 400°C in a steam of nitrogen atmosphere by Shimadzu DTG 60H thermal analyzer. The experimental conditions were: platinum crucible, nitrogen atmosphere with a 30 mL/min flow rate and a heating rate 10°C/min. Differential scanning calorimetry (DSC-TGA) analyses were carried out using SDT-Q600-V20.5-Build-15 at the Institute of Graduate Studies and Research, Alexandria University. Dielectric measurements were carried out in the frequency range from 0.1 to 5000 kHz using a Hioki 3532 LCR tester, at different temperatures ranging from room temperature up to about 90°C. The polymer powder were pressed to form discs of diameter 10 mm and thickness 1 mm. Silver electrodes were deposited on both sides of the sample surface by thermal evaporation and two copper wires were fixed on the sample using conducting silver paint. Inherent viscosities (η_{inh}) were measured at a concentration of 0.5g/dL in DMF at 30°C by using an Ubbelohde viscometer. Elemental analyses were performed at the Microanalytical Unit, Cairo University. The morphologies of polymer nanoparticles were observed by Scanning Electron Microscope (SEM) (JEOL-JSM5300), at the E-Microscope Unit; Faculty of Science, Alexandria University. The samples were sonicated in de-ionized water for 5 min and deposited onto carbon-coated copper mesh and allowed to air-dry before examination.

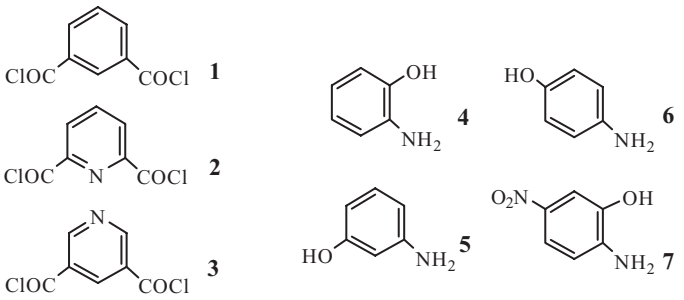

Fig. 1. Monomers used in the polycondensation process.

2.3 Polymer Synthesis

Stirring of solutions during the polycondensation reactions throughout the entire study was performed using mechanical Stirrer (600 rpm). A typical procedure was as follows. To a stirred solution of the aminophenol (**4**–**7**) (5 mmol) in NMP (25 ml) at 0°C (ice-salt bath), 4.9 mmol of the diacid chloride (**1**–**3**) was added portionwise over a period of 30 min. while stirring vigorously. The mixture was stirred at 0°C for 1 h and at rt for additional 3 h, then

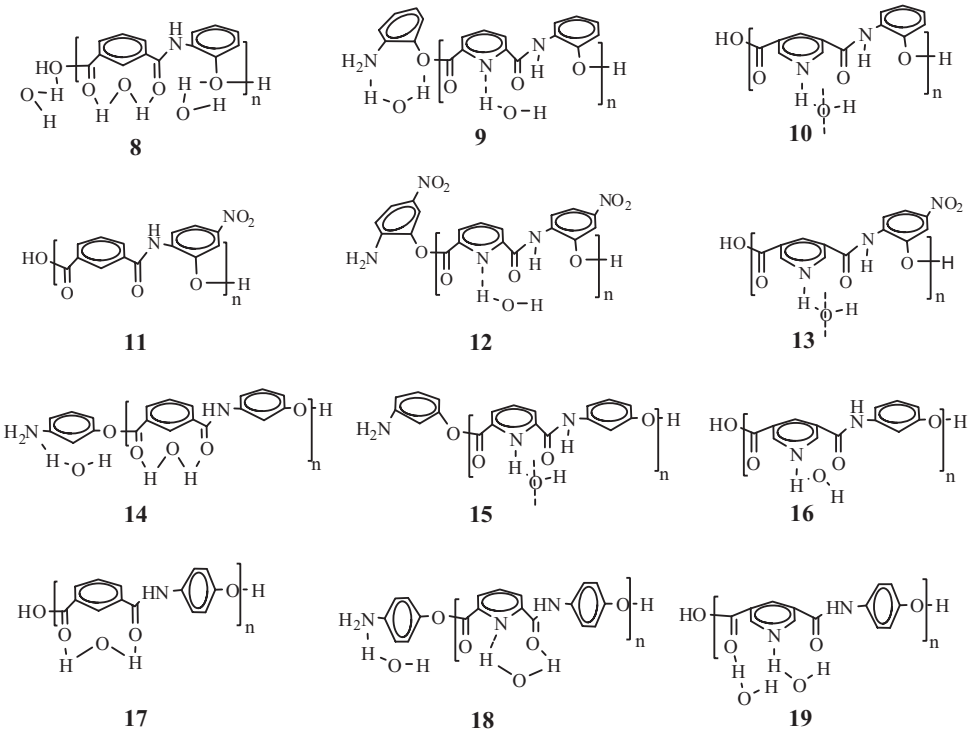

Fig. 2. Chemical Structures of the prepared polyesteramides.

it was poured into iced water. The obtained precipitate was filtered and washed thoroughly with hot methanol and hot water, and then it was dried under vacuum overnight.

2.4 Particle Preparation

The diacid chloride (**1**–**3**) (4.9 mmol) and 2-amino-5-nitro-phenol **7** (5 mmol) were each dissolved in 50 ml NMP and cooled at 0°C (ice-salt bath). Distilled water (10 mL) was added to the solution of **7** followed by addition of the entire acid chloride solution at once. The mixture was stirred vigorously at 0°C for 1 h. The polymer solution was extracted by centrifugal separation for 25 min at 15000 rpm and the greenish-yellow precipitate (∼10 % yields) was carefully washed five times with methanol and water to purify the product of any unreacted monomer. The yellow supernatant was concentrated by rotary evaporation as much as possible and the obtained yellow precipitate was filtered, washed thoroughly with methanol and water. The polymer samples were then dried at 80°C for 10 h then kept in a vacuum desiccator.

2.5 Preparation of Cu (II) Complexes Cu11−Cu13; General Method

To a stirred suspension of (0.10 mol) of the polyesteramide in 25 mL DMSO, 0.12 mol of $Cu(OAc)_2$. H_2O was added. The mixture was vigorously stirred at 90°C for 1 h, then poured while hot on a large amount of crushed ice/H_2O. The dark colored precipitate was filtered, washed with hot methanol and water and dried at 80°C for 10 h, then kept in a vacuum desiccator.

3 Results and Discussion

The production of new types of semiconducting polyesteramides containing pyridine linkages and studying of their properties is the major objective of our study. One of the most important tasks in this study is to analyze and predict the detailed polymer structure-property relationship that could increase the conjugational degree along the backbone of the polymers without much impairing their thermal stability.

Three aromatic acids chlorides, Figure 1, namely isophthaloyl dichloride **1** pyridine-2,6-dicarbonyl dichloride **2** and pyridine-3,5-dicarbonyl dichloride **3** were used in this investigation. These compounds were prepared by reactions of their corresponding dicarboxylic acids with thionyl chloride in the presence of few droplets of DMF (21). Polyesteramides (Fig. 2) were synthesized in good yields by direct polycondensation reaction of an equimolar mixture of the acids chlorides **1–3** with aminophenols including 2-aminophenol **4**, 3-aminophenol **5**, 4-aminophenol **6** and 2-amino-5-nitro-phenol **7** in NMP solution. The polymer structures were confirmed by elemental analysis and IR spectroscopy. Table 1 compiles physical properties of the prepared polymers.

Table 1. Yield (%), elemental analyses and inherent viscosity of the prepared polymers

#	*Yield (%)*	*Unit Formula*	*M.Wt*	*% C (Exp)*	*% H (Exp)*	*% N (Exp)*	η_{inh}†
8	92	$C_{14}H_{17}NO_7$	311	54.02 (55.19)	5.50 (5.40)	4.50 (3.88)	0.912
9	91	$C_{19}H_{19}N_3O_6$	385	59.22 (60.01)	4.97 (6.80)	10.90 (11.21)	0.930
10	90	$C_{13}H_{10}N_2O_4.{}^1/_2H_2O$	267	59.65 (58.97)	4.11 (5.78)	10.48 (10.92)	0.944
11	92	$C_{14}H_{10}N_2O_6$	302	55.63 (56.28)	3.33 (3.90)	9.27 9.30	0.945
12	91	$C_{19}H_{15}N_5O_9$	457	49.90 (49.71)	3.31 (4.94)	15.31 (14.47)	0.967
13	90	$C_{13}H_9N_3O_6.{}^1/_2H_2O$	312	50.00 (50.27)	3.20 (5.29)	13.46 (13.82)	0.949
14	95	$C_{20}H_{20}N_2O_6$	384	62.49 (61.40)	5.24 (6.43)	8.29 (8.61)	0.955
15	90	$C_{19}H_{15}N_3O_4.\ {}^1/_2H_2O$	358	63.68 (63.29)	4.46 (5.61)	11.73 (11.71)	0.961
16	82	$C_{13}H_{12}N_2O_5$	276	56.52 (57.39)	4.38 (6.85)	10.14 (10.58)	0.962
17	84	$C_{14}H_{13}NO_5$	275	61.09 (61.34)	4.76 (5.53)	5.09 ——	0.899
18	80	$C_{19}H_{19}N_3O_6$	385	59.22 (59.65)	4.97 (5.78)	10.90 (10.92)	0.902
19	90	$C_{13}H_{14}N_2O_6$	294	53.06 (52.97)	4.80 (5.54)	9.52 (9.19)	0.969

†The inherent viscosity of the polymers was measured at a concentration of 0.5g/dL in DMSO at 30°C.

3.1 Physical Properties Of Polymers

3.1.1. *Solubility*

The prepared pyridine-containing polyesteramides showed different solubility behaviors in different organic solvents. Moderate to complete dissolutions (5 wt% solid content) were observed at room temperature in a variety of aprotic solvents such as NMP, DMSO, DMAc, while insoluble in boiling alcoholic solvents such as methanol, ethanol, propanol and ethylene glycol or in halogenated solvents such as $CHCl_3$, CCl_4, CH_2Cl_2 or in ethers such as Et_2O, THF, 1,4-dioxane or 1,2-dimethoxyethane (DME).

3.1.2. *Inherent viscosity*

The inherent viscosity of the polymers, as a suitable criterion for evaluation of molecular weight, was measured at a concentration of 0.5 g/dL in DMF at 30°C. It was in the range of 0.899–0.967 dL/g that showed moderate molecular weights (Table 1). In general, linear symmetric polymers showed higher η_{inh} values and thus a higher degree of polymerization than those derived from non-symmetric analogues.

3.1.3. *FTIR Spectroscopy*

The FT-IR spectra of the polyesteramides exhibited characteristic absorption bands at around 3300 and 1650 cm^{-1} corresponding to the N-H and C=O stretching of amide group, respectively. The spectrum of polymers containing nitro group **11**, **12** and **13** showed characteristic bands of nitro groups at υ 1318 and 1580 cm^{-1}. The IR spectra of representative examples polymers **9**, **12**, **15**, **18** and **10**, **13**, **16**, **19** are shown in Figures 3 and 4, respectively.

3.1.4. *Optical Properties*

The optical properties of representative polymers, (Figs. 5) were investigated by UV-Vis spectroscopy in NMP with a polymer concentration of $\sim$ 2 mg/10 mL. The absorption spectra of the poly (amide-ester)s **9, 12, 15**, **18** and **10, 13, 16**, **19** are shown in Figures 5(a) and (b), respectively. Comparison between poly(amide-ester)s derived from different diacid chlorides with the same aminophenol clearly revealed that the absorption characteristics of the polymer are affected by the linear conjugated system. It is also obvious that the absorption bands of polymers derived from 2,6-pyridine dicarboxylic acid exhibit a slight red-shift than those derived from 3,5- analogues and isophthalic acid. The relatively lower $\pi - \pi^*$ transitions are likely attributed to the fact that most pyridine groups are protonated by the librated HCl during the polycondensation process. The introduction of nitro group in **11**–**13** led to a red shift in the absorption and interestingly these polymers have bright yellow colors in the solid state.

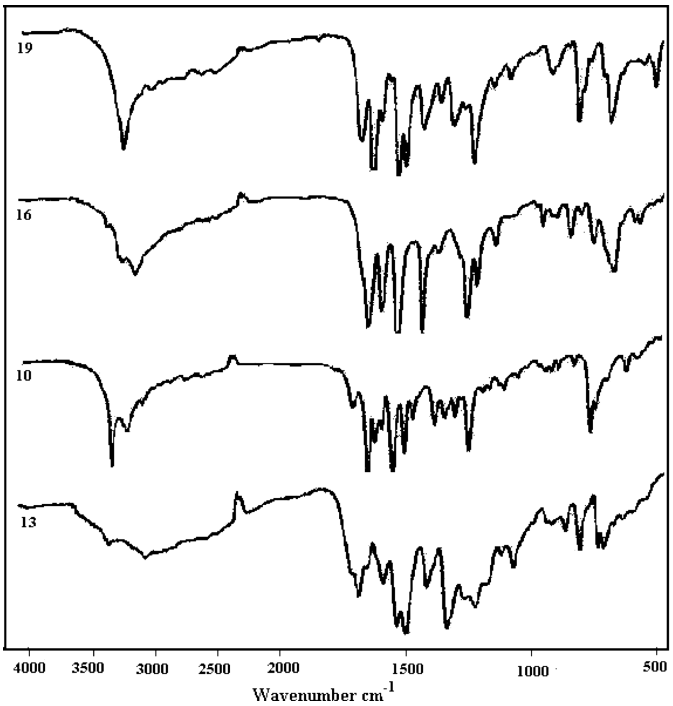

Fig. 3. IR spectra of polymers **9**, **12**, **15**, **18**.

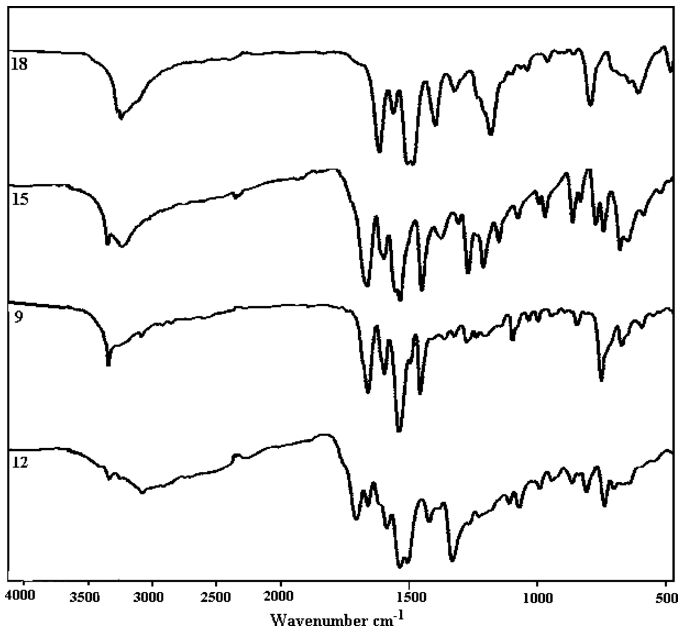

Fig. 4. IR spectra of polymers **10**, **13**, **16**, **19**.

3.1.5. *Thermal properties*

The thermal properties of the prepared polymers were evaluated by differential thermo gravimetric (DTG), differential thermal analysis (DTA) and differential scanning calorimetry (DSC) techniques. Thermal and kinetic data obtained from the nonisothermal decomposition of the investigated polymers are compiled in Table 2. Interestingly, the prepared polymers exhibited high thermal stability and most of them showed similar major amide/ester linkages degradation. Furthermore, structure-thermal property correlation based on changing the dicarboxylic acid monomer demonstrated an interesting connection between a single change and thermal properties. For instance, polymers **8–10** obtained from **4** demonstrated high thermal stability and their exothermic decomposition weight loss peaks appeared, respectively, at 380°C, 321°C and 340°C and while the remaining mass residues were 0.00%, 18.98% and 38.44%, respectively. However, introduction of the nitro group into the polymer backbone not only improved the thermal stability but also furnished polymers **11**–**13** having bright yellow colors in the solid state. The exothermic decomposition weight loss peaks of polymers **11**–**13** appeared, respectively, at 450°C, 368°C and 386°C and while the remaining mass residues were 24.70%, 36.08% and 14.36%, respectively. Polymers **14**–**16** prepared from **5** exhibited different thermal behaviors. For instance, **14** and **15** showed similar thermal decompositions up to 380°C, whereas **16** exhibited a major internal dehydration process leaving the major portion of the polymer intact. The char yields of this series were 31.44%, 55.45% and 76.41%, respectively. Polymers **17**–**19** prepared from **6** exhibited major amide linkage degradation and their thermal stabilities

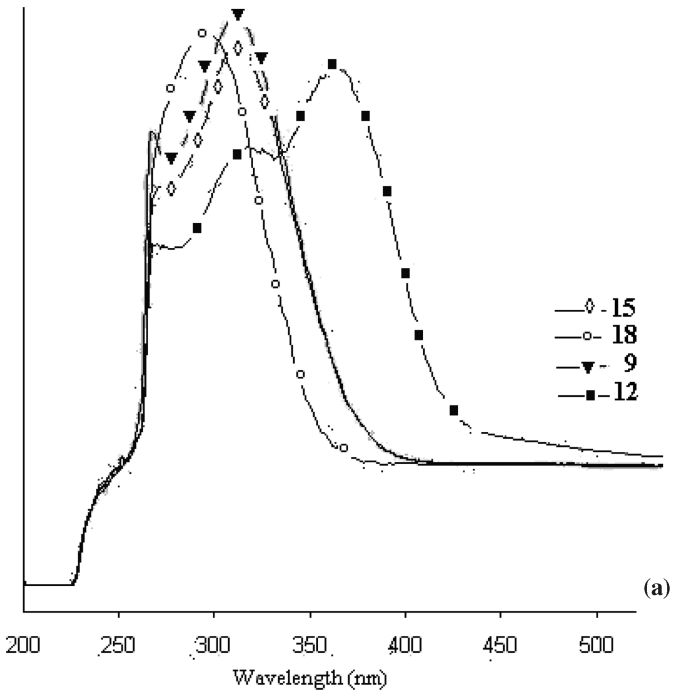

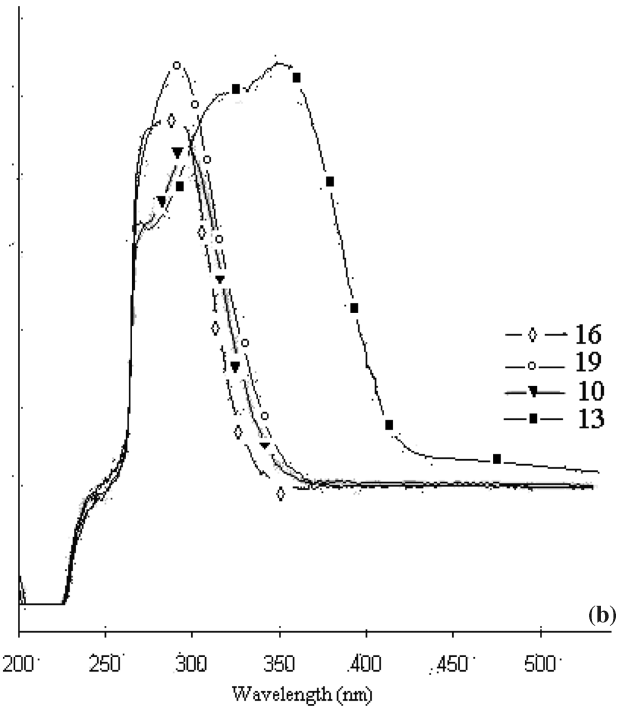

Fig. 5. Absorption spectra of polyesteramides: (a) **9, 12**, **15**, **18** and (b) **10**, **13**, **16**, **19.**

were in the order **17**>**19**>**18**, respectively. The char yields of this series were 67.28%, 48.20% and 55.50%, respectively.

The thermodynamic parameters of decomposition processes of complexes, namely, activation energy (E_a), enthalpy (ΔH^*), entropy (ΔS^*), and Gibbs free energy change of (ΔG^*) were evaluated graphically by employing the

Table 2. Thermal decomposition data of polymers **8**–**19** as recorded from their DTG curves

#	*TG (°C)*	*Wt Loss (%)*	*Residue (%)*	T^{+}	E_a *(kj/mol)*	ΔH *(kj/mol)*	ΔS *(kj/mol)*	ΔG *(kj/mol)*
8	080–200	01.84		355	11.48	8.54	–0.28	108.65
	200–550	98.07	0.00	538	22.33	17.86	–0.28	169.38
9	072–147	08.60		343	3.82	0.98	–0.29	101.49
	205–600	72.42	18.98	521	34.46	30.14	–0.28	176.63
				594	25.53	20.59	–0.28	187.23
	048–250	03.09						
10	250–600	58.52	38.44	581	9.57	4.74	–0.29	174.81
	050–190	ND						
11	200–550	74.40	24.70	558	19.14	14.50	–0.28	172.39
	213–277	39.81		486	19.15	15.11	–0.29	153.77
12	232–650	24.11	36.08	551	16.75	12.17	–0.29	171.81
				595	71.80	66.87	–0.28	236.08
				630	52.65	47.41	–0.28	224.81
	080–240	07.98		431	6.38	2.80	–0.29	129.82
13	240–650	77.64	14.36	571	38.29	33.55	–0.28	193.26
				641	28.72	23.39	–0.28	205.51
	080–200	02.18		336	15.95	13.16	–0.29	111.24
14	200–650	68.56	31.44	545	38.29	33.76	–0.17	124.77
				591	19.15	14.24	–0.05	41.43
				649	38.29	32.90	–0.30	227.86
	071–309	09.44		344	11.49	8.62	–0.30	110.29
15	350–650	35.11	55.45	535	5.22	0.77	–0.31	167.04
				638	28.72	23.41	–0.29	210.19
	062–257	03.22		335	2.61	–0.17	–0.30	101.53
16	257–650	19.37	76.41	530	0.93	–3.46	–0.07	35.16
				585	9.57	4.71	–0.30	181.15
				636	19.15	13.85	–0.17	124.54
	080–200	ND						
17	200–600	32.71	67.28	554	6.38	1.77	–0.29	163.35
	087–170	12.04		357	9.57	6.60	–0.29	110.42
18	225–650	39.67	48.2	534	25.53	21.09	–0.29	177.85
				630	19.15	13.91	–0.29	198.88
	058–291	06.38		585	9.57	4.71	–0.29	176.23
19	300–670	38.01	55.5	652	9.57	4.15	–0.30	196.83

[+]The peak temperature from the DTG charts.

Coats-Redfern method (22, 23). This method, reviewed by Johnson and Gallagher (23) as an integral method assuming various orders of reaction and comparing the linearity in each case to select the correct order by using Equations (**1**) and (**2**):

$$\log\left[\frac{1-(1-\alpha)^{1-n}}{T^2(1-n)}\right] = \log\left[\frac{AR}{\theta E_a}\left(1-\frac{2RT}{E_a}\right)\right] - \frac{E_a}{2.303RT} \quad \text{for } n \neq 1 \qquad (1)$$

$$\log\left[\frac{-\log(1-\alpha)}{T^2}\right] = \log\left[\frac{AR}{\theta E_a}\left(1-\frac{2RT}{E_a}\right)\right] - \frac{E_a}{2.303RT} \quad \text{for } n = 1 \qquad (2)$$

Where α is the fraction of sample decomposed at time t, T is the derivative peak temperature, A is the frequency factor, E_a is the activation energy, R is the gas constant, θ is the heating rate, and $(1 - (2RT/E_a)) \cong 1$. A plot of $\log[-\log(1-a)/T^2]$ vs. $1/T$ gives a slope from which the E_a was calculated and A (Arrhenius factor) was determined from the intercept. Trials of these plots were made by assuming the orders 0, 1/2, and 1 and the best plot was obtained for the first order. The entropy of activation was calculated (24) using Equation (**3**):

$$\Delta S^{*} = 2.303R\left[\log\frac{Ah}{kT}\right] \qquad (3)$$

Where h and k stand for the Plank and Boltzmann constants, respectively, and T is the peak temperature from the DTG curve. The enthalpy of activation ΔH^{*} and the free energy of activation ΔG^{*} are calculated using Equations (**4**) and (**5**), respectively.

$$\Delta H^{*} = E_a - RT \qquad (4)$$

$$\Delta G^{*} = \Delta H^{*} - T\Delta S^{*} \qquad (5)$$

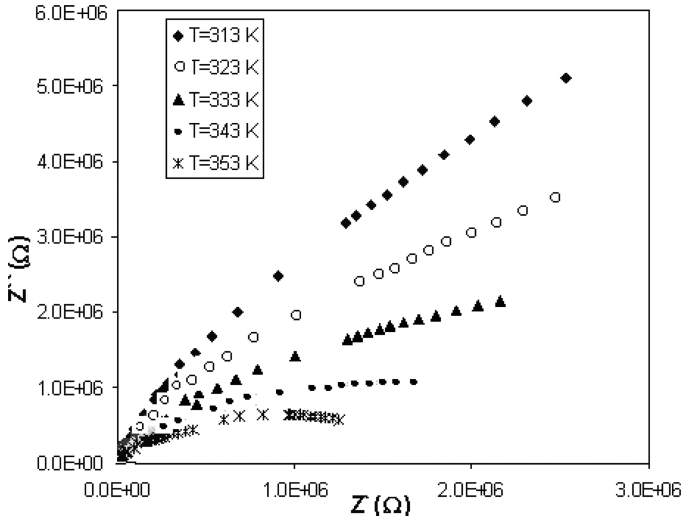

Fig. 6. Complex impedance diagram for polymer **11** conductivity at different temperatures.

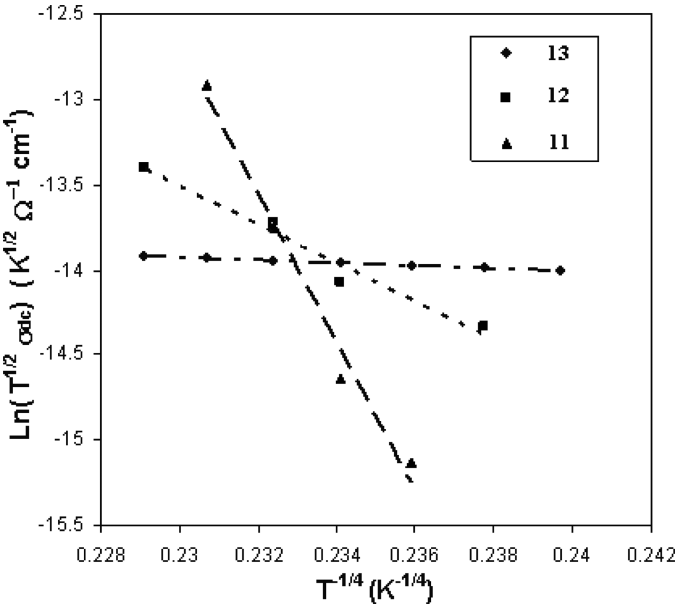

Fig. 7. Temperature dependence of the dc for polymers **11**, **12**, **13** plotted as ln $(T^{1/2}\sigma_{dc})$ vs. T^{-1}.

According to the kinetic data obtained from DTG curves all polymers have negative entropy (ΔS^*), which indicates ordered systems and more ordered activated states that may be possible through the chemosorption of other light decomposition products.

3.1.6. *Electrical properties*

The conjugated polymers have been studied for many years (25) because of their attractive electronic and optoelectronic properties. One of the most important goals is to develop narrow-band gap polymers in the field of materials science. Indeed, a narrow band gap can be obtained by starting from a monomer which already has a narrow HOMO–LUMO energy (26) separation. Hence, to find low energy gap parent molecules is the key step of designing conductive polymer. Based on this hypothesis, many studies on organic conjugated systems combine with donor–acceptor groups or fused with other conjugated ring to reduce their band gaps have been reported (27). Such data attracted interest in many areas of materials research such as in organic light-emitting displays (LEDs), field-effect transistors (FETs), solar cells and switching devices and so forth.

The dc electrical conductivity results of polymers **8–19** revealed different behavior. The relations between the real (Z') and imaginary (Z") parts of the impedance at different temperatures were plotted for the mentioned samples. Figure 6 represents the Z"-Z' for **11** as a representative graph and similar graphs were obtained for other polymers. The behavior of the Cole-Cole diagrams is characterized by semicircles originating from the origin with no overlap at all temperatures. Extrapolating the high frequency limit of the semicircles intercepts the real axis Z' giving the value of the bulk resistance for the sample from which the dc conductivity was calculated. The temperature dependence versus dc conductivity for polymers **11–13** plotted as ln $T^{1/2}\sigma_{dc}$ vs. $T^{-1/4}$ is presented in Figure 7.

Interestingly, the dc conductivity of pyridine-containing polymers **9**, **10**, **12**, **13**, **15**, **16**, **18** and **19** increases with increasing temperature as determined from the polt of ln (σ) vs. 1/T. This behavior is indicative of semi-conducting nature of these samples as it obeys the three dimensional Mott variable-range hopping model (27) which describes the temperature dependence of the conductivity of disordered semiconducting materials and provides the best fitting for $\sigma_{dc}(T)$ as given in Equation 6:

$$\sigma_{dc}(T) = \sigma_o T^{-1/2} \exp\left[-\left(\frac{T_o}{T}\right)^{1/4}\right] \qquad (6)$$

However in the case of other phenylene-containing polymers **8**, **11**, **14** and **17**, no variation of the conductivity with the temperature was observed for the studied

Table 3. Electrical conductivity (σ) for polymers **8–19** at 330 K in Ω^{-1} cm^{-1}

	σ (Ω^{-1} cm^{-1})		σ (Ω^{-1} cm^{-1})		σ (Ω^{-1} cm^{-1})		σ (Ω^{-1} cm^{-1})
8	4.25×10^{-9}	**11**	4.76×10^{-8}	**14**	5.23×10^{-7}	**17**	1.87×10^{-7}
9	2.14×10^{-8}	**12**	2.04×10^{-8}	**15**	1.43×10^{-7}	**18**	2.19×10^{-7}
10	2.09×10^{-8}	**13**	4.04×10^{-8}	**16**	1.54×10^{-7}	**19**	1.23×10^{-7}

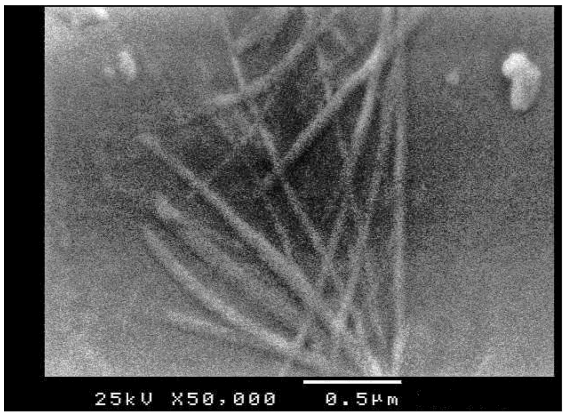

11A

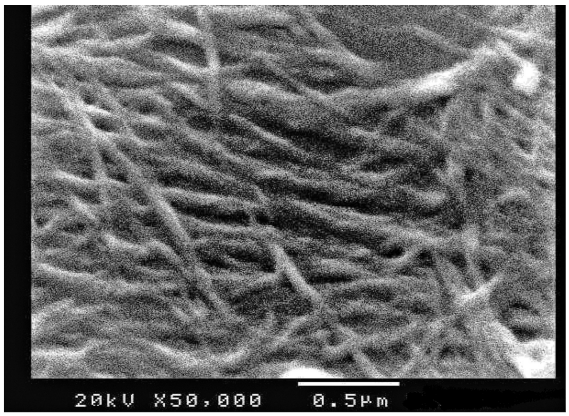

11B

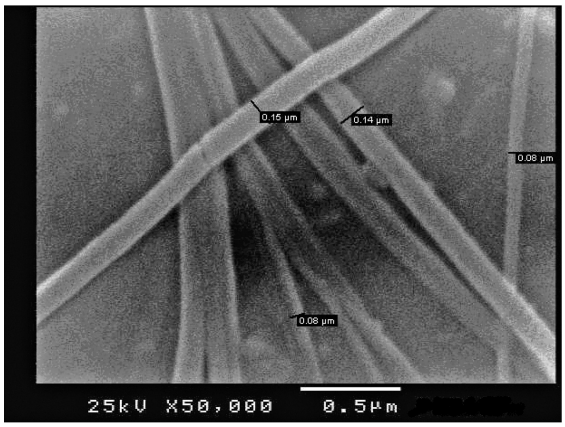

12A

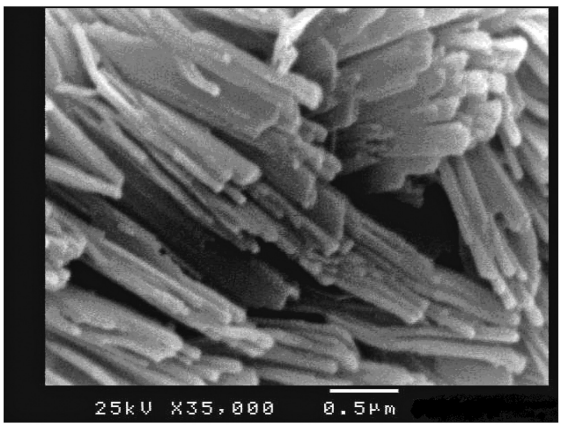

12B

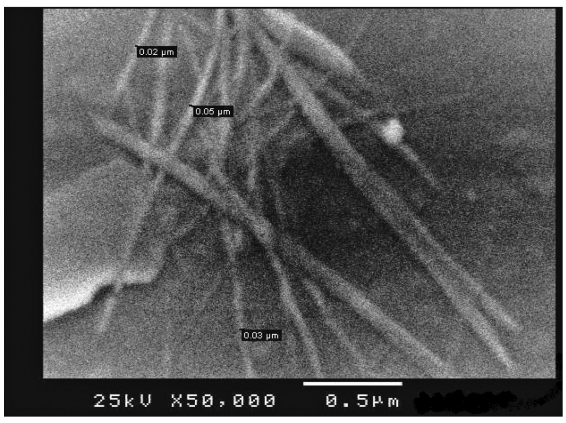

13A

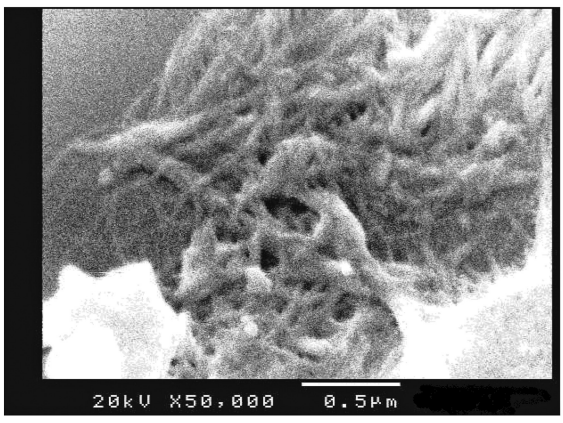

13B

Fig. 8. SEM images of **11A**–**13A**: precipitate of the produced particles in 10% aqueous NMP after 25 min centrifugation (15000 rpm) and **11B**–**13B**: particles aggregates obtained by evaporation of the supernatant.

temperature range. The dc conductivity values of polymers **8**–**19** at 330 K are listed in Table 3.

3.2 Preparation and Characterization of Polyesteramides Nanoparticles

Developing novel semiconducting nanoparticles made from organic polyesteramides and their metallic complexes was our next research interest. Polymeric aromatic nanoparticles can be prepared by either emulsion or interfacial polymerizations. Biodegradable polyesters and their copolymers nanoparticle preparation can be achieved using emulsification/solvent evaporation, emulsification/solvent diffusion and salting out techniques (28). Additionally, a popular method used for polymeric nanoparticles preparation is solvent displacement also referred as nanoprecipitation (29). This method involves the dissolution of the monomers in an organic, water-miscible solvent, which is then added to the aqueous phase in the presence or absence of a surfactant. Upon addition to the aqueous phase, the organic solvent immediately diffuses out leading to the formation of nanoparticles. Polyesteramides nanoparticles **11**–**13** were synthesized in good yields by direct polycondensation of an equimolar mixture of the specific acid chloride with 2-amino-5-nitrophenol in 10% aqueous NMP at 0°C for 1 h. The entire polycondensation reactions readily proceeded in homogenous solutions that were subjected to centrifugal separation for 25 min at 15000 rpm to produce ~10% of **11**–**13** as well-separated rod-like nanoparticles polymers. Rotary evaporation of the yellow supernatants to small volumes furnished the major yields of interconnected particles **11**–**13**. Interestingly, the diameters of particles obtained by centrifugation were comparable with that particles obtained by concentration of the supernatant as judged from SEM images (Fig. 8). NMP served a dual purpose as a solvent and to remove HCl generated during the polymerization, because HCl not only hinders the polymerization reaction, resulting in a lower molecular weight product, but it also would catalyze the hydrolysis of the polymeric product. NMP was described as an athermal solvent for nanotubes by Bergin et al. (30). Mixing NMP with 10% H_2O was essential for many reasons such as controlling the particles morphology, playing important role in determining the polarity of the reaction solution and as a reaction accelerator (31).

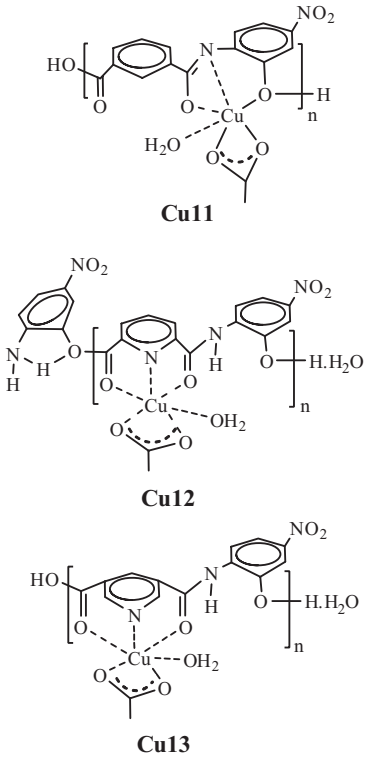

Fig. 9. Proposed chemical structures of the prepared polyesteramides copper (II) complexes.

Figure 8 displays scanning electron microscope (SEM) images **A** of the greenish-yellow precipitates of the produced particles after centrifugation and images **B** of the particles aggregates obtained by evaporation of the yellow supernatant. The average diameters of polymers **11** and **13** were 40 nm, while polymer **12** rods were wider and their average width was 112 nm. The formation mechanism of polymers is related to effect of salts ions on the micelle structure. Micelles grow in the presence of salts from spherical, rodlike to cylindrical aggregates or wormlike micelles (32). The morphological transition from spherical to cylindrical morphology may be attributed to the existent salt ions such as $NMPH^+Cl^-$ and H_3O^+ in reaction medium. The large diameter recorded for polymer **12**, in comparison to analogues **11** and **13**, is owing to the presence of a relatively higher number of H-bonding interactions (33) which also illustrate the tendency of such large diameters to flatten.

Table 4. Physical properties of the prepared copper (II)-polymers complexes **(Cu11−Cu13)**

#	*Yield (%)*	*Unit Formula*	*M.Wt*	*% C (Exp)*	*% H (Exp)*	*% N (Exp)*	*Selected IR bands (cm^{-1})*	*Color*
Cu11	95	$C_{16}H_{14}N_2O_9Cu$	441.5	43.48 (42.66)	3.17 (2.27)	6.34 (7.12)	3380, 1630, 1597, 1508, 1345, 1080	Dark Brown
Cu12	95	$C_{21}H_{20}N_5O_{12}Cu$	597.5	42.18 (41.99)	3.37 (2.59)	11.71 (11.71)	3400, 1630, 1592, 1328, 1078, 678	Brown
Cu13	94	$C_{15}H_{16}N_3O_{10}Cu$	461.5	39.01 (38.85)	3.49 (2.51)	9.10 (9.96)	3347, 1633, 1595, 1344, 1077, 680	Brown

3.3 Preparation of Polyesteramides-copper (II) Complexes

Polyesteramides **11**–**13** took the center stage with the performance as these materials were obtained in a bright-yellow color, which is unusual with this polymer group, and their properties can be tuned for specific application such as self-coated semiconducting material. Therefore, incorporation of a transition metal to these polymers group was our next goal. The complexation reaction was carried out by careful addition of $Cu(OAc)_2$. H_2O (1.2 equivalent) to the stirred hot solution of the polymer in DMSO at (80–90°C) for 1 h. The Cu (II) ions were complexed with polymer repeating unit in a ratio of 1:1 and the complexes structures **Cu11**−**Cu13** given in Figure 9 are proposed on the basis of their IR and elemental analyses data (Table 4). Pyridine-containing polymers **12** and **13** showed similar sites of metal coordination. The metal ion accommodates inside the inner cavity made by the protonized pyridine nitrogen atom (H-O-H—NC_5H_5) with the two surrounding carbonyl groups. The appearance of the sharp (Cu-N) bands at υ 678 and υ 680 cm^{-1} in complexes **Cu12** and **Cu13**, respectively, unambiguously proved that the pyridine nitrogen atom represents the central binding site, followed by axial orientation of bonds connecting pyridine and CO amide-ester groups. All prepared complexes showed chelating bidentate CH_3COO^- bands around 1528 and 1455 cm^{-1}. These two bands are due to υ_{as} (COO^-) and υ_s (COO^-), respectively. The separations of these two bands $\Delta\upsilon = \upsilon_{as} - \upsilon_s = 73$ cm^{-1}, are comparable to the values cited for the bidentate character(34) of the acetate group. In comparison with the IR spectra of polymers **11**–**13**, all the complexes **Cu11**−**Cu13** exhibit downshift (~30 cm^{-1}) of υ(CONH) indicating the participation of the amide CO in the coordination to the metal ion. The presence of coordinated water molecules in the complexes(35) is indicated by a broad band centered on υ 3400 cm^{-1} and two weak bands in the region 750–800 and 700–720 cm^{-1} due to υ (-OH) rocking and wagging mode of vibrations, respectively (36).

The electronic spectra of the complexes were investigated by UV-vis spectroscopy in DMSO with polymers concentrations of 10^{-3} M, (Fig. 10). The maximum absorptions λ_{max}) and absorption values (A) of ligands **11**–**13** and their corresponding copper (II) complexes **Cu11**–**Cu13** are compiled in Table 5. The prepared polyesteramides exhibited three bands at λ_{max} around 269, 315 and 362 nm due to the $\pi - \pi^*$, $n - \pi^*$ and charge transfer transitions, respectively, within the molecule. The absorption characteristics of the polymer are affected by the linear conjugated system. This result clearly showed that polymer **12**, derived from 2,6-pyridine dicarboxylic acid, exhibits a slight red-shift than its partners **13** and **11** derived from 3,5-pyridine dicarboxylic and isophthalic acids, respectively. The slight red-shifts observed in the transitions occur in **12** and **13** are likely attributed to the protonized pyridine nitrogen atom by water (O-H—NC_5H_5) (37).

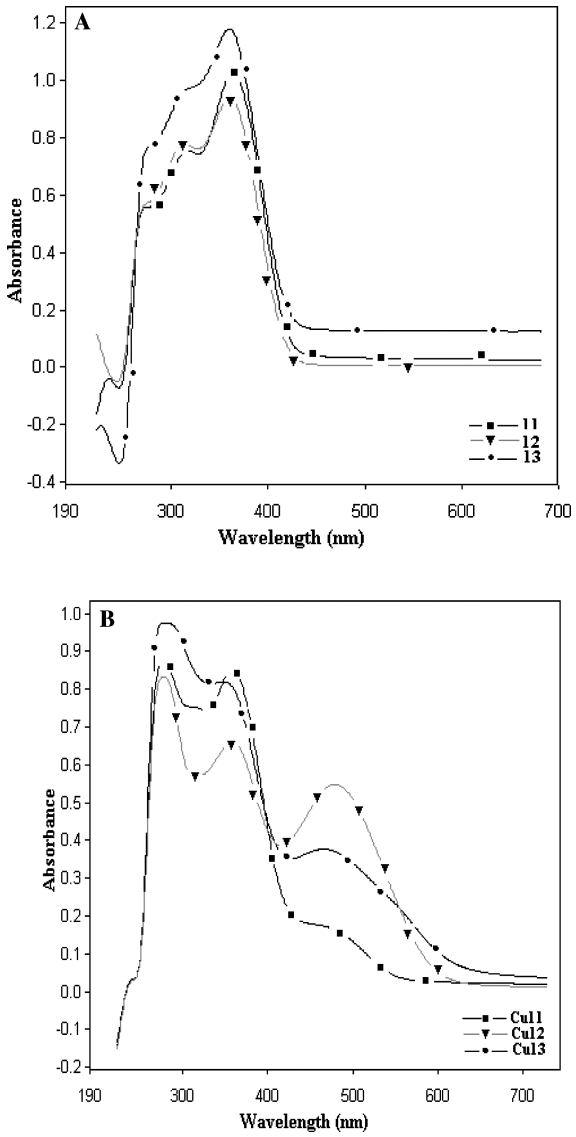

Fig. 10. Absorption spectra of polyesteramides **11**–**13** (**A**) and their complexes **Cu11**–**Cu13** (**B**).

The electronic spectra of the complexes showed, in addition to the three aforementioned transitions, a new band at 465 nm, 480 nm, and 480 nm for **Cu11**, **Cu12** and **Cu13** which is attributed to the ligand-metal charge transfer (LMCT) transitions from the conjugated *n*- and *p*-orbitals of the donor to d orbitals of the metal. The expected d-d transition bands of the prepared copper polymers were found as shoulders around 560 nm (38).

The thermal properties of the prepared polymers were evaluated by differential thermo gravimetric (DTG), differential thermal analysis (DTA) and differential scanning calorimetry (DSC) techniques. The postulated thermal degradation analyses of the prepared copper complexes **Cu11**–**Cu13** are shown in Figure 11. Interestingly, all polymers complexes exhibited similar thermal decompositions up to 390°C and the remaining residues yields of

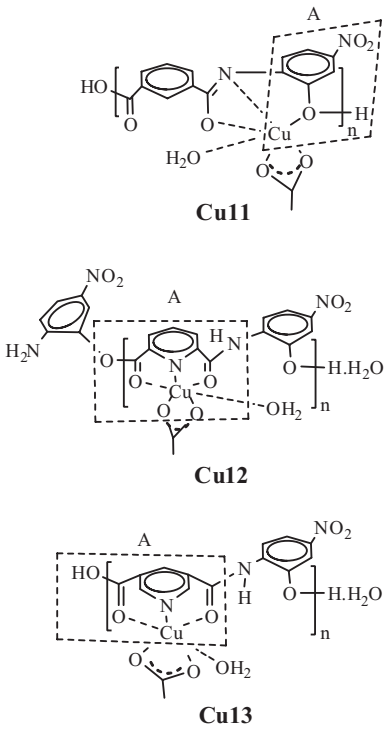

Fig. 11. The postulated thermal degradation of polymers **Cu11**–**Cu13**.

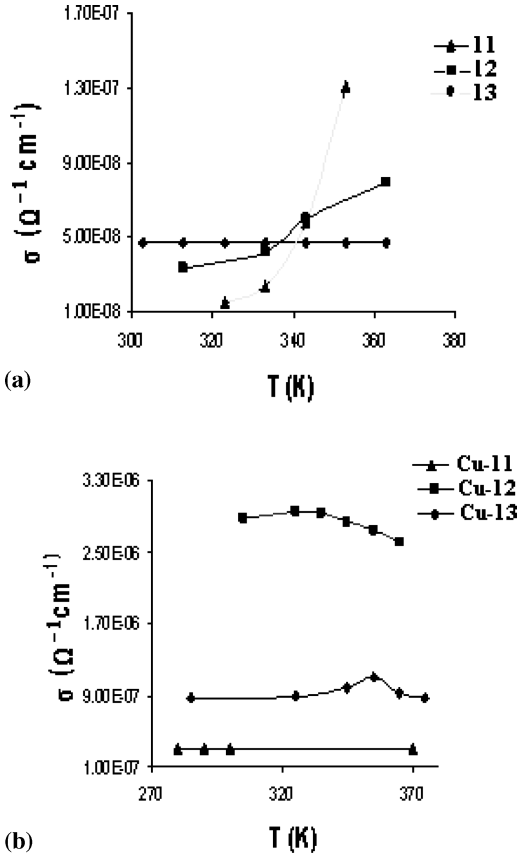

Fig. 12. (a) Temperature dependence of dc electrical conductivity for polymers **11**–**13,** (b) Temperature dependence of dc electrical conductivity for polymers **Cu11**–**Cu1**.

this series were 45.25%, 43.92% and 46.76%, respectively, attributed to their corresponding fragments A and these results further supplement the proposed compositions of the complexes.

The incorporation of copper into the polymers backbones significantly improved the dc conductivities of the resulted complexes. The temperature dependence versus dc conductivity for the copper complexes **Cu11-Cu13** plotted as σ (Ω^{-1} cm^{-1}) vs. T (K) is presented in Figure 12 and their conductivity values are listed in Table 6. The conductivity of the complex **Cu12** exhibited nearly a seventy three orders of magnitude higher than that of its ligand **12**. The complex exhibits a semiconducting character at 300–330 K range changed to a metallic character at T > 330 K. In a similar fashion, **Cu13** exhibits a semiconducting character below 350 K changed to a metallic character at higher temperatures and in addition, its conductivity is nearly two orders of magnitude higher than that of ligand **13**. In case of **Cu11**, the conductivity revealed a five orders of magnitude improvement compared to **11** but it does not change with increasing temperature. It is obvious that the polymer structural variations play a major role in determining the electrical conduction efficiency of the complexes **Cu11**−**Cu13**.

The complexation of polymers **11**–**13** with hydrated $Cu(OAc)_2$ produce charge-transfer complexes which would give an effective contribution to the electrical conductivity of the polymer. The charge carriers in complexes **Cu12** and **Cu13** are generated by activation of the *n*-electrons of the pyridine N-atom after doping with Cu $(OAc)_2.H_2O$. It is well known that conjugated polymers undergo oxidation and reduction from their electrically neutral, nonconductive state, with the formation of highly conductive

Table 5. λ_{max} and absorption values (A) of polymers **11**–**13** and their corresponding copper complexes

	11	**12**	**13**	**Cu11**	**Cu12**	**Cu13**
λ_{max}	362 (0.940)	360 (1.179)	364 (1.029)	465 (0.377)	480 (0.162)	480 (0.548)
(A)	314 (0.779)	316 (0.972)	314 (0.759)	349 (0.820)	360 (0.854)	358 (0.661)
	268 (0.551)	270 (0.732)	268 (0.545)	286 (0.974)	314 (0.756)	280 (0.827)
				270 (0.950)	280 (0.867)	

Table 6. Electrical conductivity (σ) for polymers **11**–**13** and the complexes **Cu11**–**Cu13** at 330 K in Ω^{-1} cm^{-1}

#	σ (Ω^{-1} cm^{-1})	#	σ (Ω^{-1} cm^{-1})
11	2.04×10^{-8}	**Cu11**	1.02×10^{-7}
12	4.04×10^{-8}	**Cu12**	2.95×10^{-6}
13	4.76×10^{-8}	**Cu13**	1.08×10^{-7}

p- and n-doped states. The introduction of units with a high electron affinity directly onto the polymeric backbone of the parent conjugated polymer is a newly developed concept to increase the efficiency and lifetime of organic conducting polymer (39). Both polymer structures are conjugated and thus, have the possibility of continuous overlap of the *n*- and *p*-orbitals throughout the entire structures. In **Cu12** and **Cu13** polymers, the Cu^{+2} ion accommodates inside the inner cavity made by the pyridine nitrogen atom with the two surrounding carbonyl groups producing two fused five- and six-membered chelate rings, respectively. The five membered ring chelates are thermodynamically more stable than six-membered chelate rings and thus, one might expect a higher mobility ligand-metal-ligand charge transfer in the former chelate ring size than the latter one. This would explain the higher conductivity of the complex **Cu12** nearly a twenty seven orders of magnitude higher than that **Cu13**.

4 Conclusions

New thermally stable polyesteramides have been successfully prepared by condensation of aromatic acids chlorides namely; isophthaloyl, pyridine-3,5-dicarbonyl and pyridine-2,6-pyridine-dicarbonyl dichlorides with the aminophenol isomers in NMP. The prepared pyridine-containing polymers exhibit semi-conducting nature as their conductivities increase with increasing temperature. No variation of the conductivity with the temperature was monitored within the studied temperature range for other phenylene-containing polymers. Introduction of the nitro group into the polymer backbone led to a red shift in the absorption and the obtained polymers have a bright yellow color, which is unusual with this polymer group, and thus polymers **11**–**13** were elected for further studies to improve their optical and electrical properties for possible specific applications. Nanometer-sized rodlike polyesteramids **11**–**13** have been successfully prepared via polycondensation/centrifugation in 10% aqueous NMP and the morphology of produced polymer nanoparticles were studied by SEM. Copper (II) ions were complexed with these polymers in a (1:1) ratio. Based on polymer structural variations, the incorporation of copper into the polymers backbones significantly improved the optical properties and the dc conductivities. The dc electrical conductivity results of the polyesteramides revealed different behaviors. Complexes of pyridine-containing polymers exhibit semiconducting characters around 330 K changed to metallic characters at higher temperatures and their conducivities increased tens of magnitudes higher than that of their corresponding ligands. The high mobility ligand-metal charge transfer in such thermally stable chelated ring sizes would explain their high conductivity. These new types of polymeric materials and their nano-sized rods may have numerous applications in nanotechnology and their properties can be tuned for specific applications such as conducting adhesives and coating materials.

Acknowledgments

Financial support by Alexandria University-Research Enhancement Program (ALEXREP) grant no. (HLTH-08-01) is gratefully acknowledged.

References

1. a) Preston, J. In Encyclopedia of Polymer Science and Technology, Mark, H.F.; Bikales, N.M., Overberger, C.G., Menges, G., Eds., Wiley Interscience: New York, Vol. 111, p. 381, 1988; b) Lin, J., Sherrington, D.C. (1994) *Adv. Polym. Sci.*, 111, 177–181.
2. a) Mathiowitz, E. and Cohen, M.D. (1989) *J. Membr. Sci.*, 40, 27–41.; b) Bulte, A.M.W., Folkers, B., Mulder, M.H.V. and Smolders, C.A. (1993) *J. Appl. Polym. Sci.*, 50, 13–26; c) Li, X.G., Huang, M.R. (1999) *J. Appl. Polym. Sci.*, 71, 565–571.
3. a) Hearle, J.W.S. High Performance Fibers. Woodhead Publishing Ltd.: Cambridge, UK, 2001; b) Nelson, G.L., Wilkie, C.A. Fire and Polymers. American Chemical Society, Washington, D.C., 2003.
4. Tashiro, K. and Yoshioka, Y. (2004) *Polymer*, 45, 4337–4348.
5. a) Yang, C.P., Hsiao, S.H. and Yang, C.C. (1997) *J. Polym. Sci., Part A: Polym. Chem.*, 35, 2147–2156, b) Zhu, Y., Zhao, P., Cai, X., Meng, W.D., Qing, F.L. (2007) *Polymer*, 48, 3116–3124, c) Kurose, T., Yudin, V.E., Otaigbe, J.U., Svetlichnyi, V.M. (2007) *Polymer*, 48, 7130–7138.
6. a) Li, T.L. and Hsu, S.L.C. (2007) *Eur. Polym. J.,* 43, 3368–3373; b) Faghihi, Kh. and Mozaffari, Z. (2008) *J. Appl. Polym. Sci.*, 108, 1152–1157.
7. a) Mikroyannidis, J.A. (2000) *J. Polym. Sci. Part A: Polym. Chem.,* 38, 2492–2503; b)Nery, L., Lefebvre, H. and Fradet, A. (2005) *J. Polym. Sci. Part A: Polym. Chem.*, 43, 1331–1341.
8. Ataei, S.M. (2005) *Eur. Polym. J.*, 41, 65–71.
9. Sek, D. and Wolinska, A. (1989) *Eur. Polym. J.*, 25, 9–14.
10. Serrano, P.J.M., Van De Werff, B.A. and Gaymans, R.J. (1998) *Polymer*, 39, 83–92.
11. Goodman, I. and Sheahan, R.J. (1990) *Eur. Polymer J.*, 26, 1081–1088.
12. a) Tsamantakis, A. and Carriere, F. (1982) *Angew. Makromol. Chem.*, 104, 19–30; b) Chau, N., Matsuda, S., Iwakura, Y. (1979) *Makromol. Chem.,* 180, 1435–1440.
13. Holden, G., Legge, N.R., Quirk, R., Schroeder, H.E. Thermoplastic Elastomers. Hanser: New York, 1996.
14. Miller, J.A., Lin, S.B., Kirk, K.S., Hwang, K.S., Wu, K.S., Gibson, P.E. and Cooper, S. (1985) *Macromolecules*, 18, 32–44.
15. Gaymans, R.J. and de Haan, J.L. (1993) *Polymer*, 34, 4360–4364.
16. Ng, H.N., Allegrezza, A.E., Seymour, R.W. and Cooper, S.L. (1973) *Polymer,* 14, 255–61.
17. Harrell, L.L. (1969) *Macromolecules*, 2, 607–12.

18. Ando, R.A., do Nascimento, G.M., Landers, R. and Santos, P.S. (2008) *Spectrochim. Acta, Part* A, 69, 319–326.
19. Jain, S.L., Bhattacharyya, P., Milton, H.L., Slawin, A.M.Z., Crayston, J.A. and Wollines, J. D. (2004) *Dalton Trans*., 862–871.
20. Balzani, V., Ed. Electron Transfer in Chemistry, Volume I-V, Wiley: Weinheim, 2001.
21. a) Ge, Z., Yang, S., Tao, Z., Liu, J. and Fan, L. (2004) *Polymer*, 45, 3627–3635; b) Tamami, B. and Yeganeh, H. (2002) *Eur. Polym. J*., 38, 933–940.
22. Coats, A.W. and Redfern, J.P. (1964) Nature, 201, 68–69.
23. Johnson, D.W. and Gallagher, P.K. (1972) *J. Physical Chem.,* 76, 1474–1479.
24. Glasstone, S. Textbook of Physical Chemistry. Macmillan: Bombay, India, 2nd Ed.; 1974.
25. Skotheim, T.A., Elsenbaumer, R.L., Reynolds, J.R. Handbook of Conducting Polymers. Marcel-Dekker: New York, 1998.
26. Tanaka, S. and Yamashita, Y. (1997) *Synth. Met*., 84, 229–230.
27. Mott, N.F., Davis, E. Electronic Processes in Non-Crystalline Materials, Clarendon Press: Oxford, 1979.
28. a) Okubo, M., Fujibayashi, T. and Terada, A. (2005) *Colloid. Polym. Sci*., 283, 793–798; b) Yuem, J.H. and Deng, Y. (2005) *Colloid. Polym. Sci.,* 283, 1172–1179.
29. a) Reis, C.P., Neufeld, R. J., Ribeiro, A.J. and Veiga, F. (2006) *Nanomedicine*, 2, 8–21; b) Galindo-Rodriguez, S., Allemann, E., Fessi, H. and Doelker, E. (2004) *Pharm. Res*., 21, 1428–1439.
30. Bergin, S.D., Nicolosi, V., Streich, P. V., Giordani, S., Sun, Z.; Windle, A.H., Ryan, , P., Niraj, P.P. Wang, Z-.T., Carpenter, L., Blau, W.J., Boland, J.J., Hamilton, J.P. and Coleman, J.N. (2008) *Adv. Mat*., 20, 1876–1881.
31. Yoshioka, Y., Asao, K., Yamamoto, K. and Tachi, H. (2007) *Macromol. React. Eng*., 1, 222–228.
32. a) Kumar, S., Naqvi, A.Z., Kabir-ud-Din. (2000) *Langmuir*, 16, 5252–5256; b) Jang, J. and Bae, J. (2004) *Angew. Chem. Int. Ed.,* 43, 3803–3806.
33. He, C., Tan, Y. and Li, Y. (2003) *J. Appl. Polym. Sci*., 87, 1537–1540.
34. Alcock, N.W., Tracy, V.M. and Waddington, T.C. (1976) *J. Chem. Soc. Dalton Trans.*, 2243–2246.
35. Singh, G., Singh, P.A., Singh, K., Singh, D.P., Handa, R.N. and Dubey, S.N. (2002)*Proc. Natl. Acad. Sci. Ind.*, 72A, 87–94.
36. Shukla, P.R., Singh, V.K., Jaiswai, A.M. and Narain, J. (1983) *J. Indian Chem. Soc.,* 60, 321–324.
37. Chen, S., Hu, J., Yuen, C.-W. and Chan, L. (2009) *Polymer*, 50, 4424–4428.
38. a. Ruiz, R., Sanz, J., Lloret, F., Julve, M., Faus, J., Bois, C. and Munoz, M.C. (1993) J. Chem. Soc. Dalton Trans, 3035–3039; b) Karaboecek, S. and Karaboecek, N. (1997) *Polyhedron*, 11, 1771–1774.
39. Levi, M.D. and Aurbach, D. (2008) *J. Power Sources*, 180, 902–908.